

Asynchronous states in networks of pulse-coupled oscillators

L. F. Abbott and Carl van Vreeswijk

Department of Physics and Center for Complex Systems, Brandeis University, Waltham, Massachusetts 02254

(Received 29 December 1992)

We use a mean-field approach to analyze the stability of the asynchronous state in a population of all-to-all, pulse-coupled, nonlinear oscillators. We determine the conditions that must be satisfied by the time constants and phase dependence characterizing the coupling between the oscillators in order for the asynchronous state to be stable. We also consider the effects of noise. This work complements results on synchronous states in similar models and allows us to study the validity of firing-rate models commonly used for neural networks.

PACS number(s): 87.10.+e, 05.90.+m, 03.20.+i

I. INTRODUCTION

Synchronization in systems of coupled nonlinear oscillators is an interesting and well-studied phenomenon [1–10]. Asynchronous states have received less attention [11,12], although, in some situations, they may be of greater importance. For example, in a healthy piece of brain tissue, many neurons (which can be modeled as nonlinear oscillators) can fire without the large-scale synchronization characteristic of epileptic activity [13] despite the large amount of excitatory coupling between neurons. Inhibition undoubtedly plays an important role in preventing large-scale synchronization [14]. However, it is of interest to identify additional elements and mechanisms that allow stable asynchronous firing.

Synchronization of oscillators has been studied in both phase-coupled [1–7] and pulsed-coupled models [8–10]. Pulse-coupled oscillators are particularly prone to synchronization [9] or near synchronization [15], although other firing patterns have been noted [16,17]. Pulse-coupled oscillators are of greater relevance for neuroscience applications since synaptic coupling is often spike mediated. We will consider a population of “integrate-and-fire” oscillators with all-to-all pulse coupling of various forms and determine the conditions under which the asynchronous state can be stable. Although the integrate-and-fire model is not a very accurate representation of a neuron, it does incorporate the pulse coupling typical of spike-mediated synaptic transmission in neural systems. In the analysis, we make use of mean-field techniques applied recently to this problem by Treves [18].

Besides its general interest, there is another important reason to study the asynchronous state. Most theoretical work on neural networks uses the average firing rate of a population of neurons as a basic dynamic variable [19–23]. This approach assumes that the relative timing of spikes is not important so that the average firing rate provides an adequate description of the activity of the neurons. A firing-rate model will work best if the population settles quickly into an asynchronous state and would be inappropriate if, for example, there is important temporal structure in the spiking. To establish the domain of validity of the widely used firing-rate models we need to determine the conditions under which a population of

neurons will fire asynchronously and to compute the relaxation times for transients about this state.

II. MODEL

The model we consider consists of N identical oscillators with uniform all-to-all coupling. We work exclusively in the large- N limit. The state of an oscillator labeled by the index i is described by a state variable x_i that runs between zero and one and satisfies the equation

$$\frac{dx_i}{dt} = F(x_i) + G(x_i)E(t). \quad (2.1)$$

The function F characterizes the behavior of the oscillator in the absence of coupling and is an arbitrary positive-definite function. G determines the dependence of the coupling on x_i and $E(t)$ is a dynamic variable characterizing the inputs coming from the other oscillators in the population. The sign of G determines whether the coupling is excitatory or inhibitory.

Equation (2.1) determines the behavior of x_i in the range between zero and one. When x_i reaches the value one, it is immediately reset to zero. This resetting corresponds to the firing of a pulse and results in a contribution to the coupling variable $E(t)$. In order to consider the effects of arbitrary rise and fall times in the coupling between oscillators, we set the response for a single pulse equal to the difference of two exponentials. If oscillator i reaches $x_i = 1$ at time t_0 , x_i is reset to zero and $E(t)$ is incremented by an amount

$$E(t) \rightarrow E(t) + \frac{\alpha_1 \alpha_2}{(\alpha_2 - \alpha_1)N} (e^{\alpha_1(t_0 - t)} - e^{\alpha_2(t_0 - t)}) \quad (2.2)$$

with α_1 and α_2 arbitrary constants except that $\alpha_2 > \alpha_1$. In the limit $\alpha_2 \rightarrow \alpha_1 = \alpha$ this becomes the familiar α -function response

$$E(t) \rightarrow E(t) + \frac{\alpha^2}{N} (t - t_0) e^{\alpha(t_0 - t)}. \quad (2.3)$$

If $\alpha_2 \rightarrow \infty$ the response becomes a single exponential decay from an instantaneous step. Because N is large we do not remove the self-coupling term in these equations (its relative contribution is of order $1/N$). This is equivalent

to a mean-field approximation.

The asynchronous state we wish to study is characterized by a coupling function $E(t)=E_0$ that is time independent corresponding to asynchronous pulsing. If we assume that the oscillators pulse at a constant, single-oscillator rate R (or, equivalently, a rate NR for the total population) then, from Eq. (2.2), we have

$$E(t)=E_0 = \int_{-\infty}^t dt' \frac{\alpha_1 \alpha_2 R}{(\alpha_2 - \alpha_1)} (e^{\alpha_1(t-t')} - e^{\alpha_2(t-t')}) = R. \quad (2.4)$$

Thus E_0 is the steady-state, single-oscillator pulsing or firing rate. Integrating Eq. (2.1) over one period $1/E_0$ between firings we find that E_0 must satisfy

$$\frac{1}{E_0} = \int_0^1 \frac{dx}{F(x) + E_0 G(x)}. \quad (2.5)$$

This equation always has a solution (for $F > 0$) if F and G are continuous with bounded derivatives unless $G > 0$ and $\int_0^1 dx/G(x) < 1$. We will study the stability of this solution.

To analyze the asynchronous state it is convenient to make a change of variables, replacing x_i by

$$y_i = \int_0^{x_i} \frac{E_0 dx}{F(x) + E_0 G(x)}, \quad (2.6)$$

which varies between zero and one and satisfies the equation

$$\frac{dy_i}{dt} = E_0 + \Gamma(y_i)\epsilon(t) \quad (2.7)$$

where

$$\epsilon(t) = E(t) - E_0 \quad (2.8)$$

and

$$\Gamma(y) = \frac{E_0 G(x)}{F(x) + E_0 G(x)}. \quad (2.9)$$

The description in terms of the variable y is completely equivalent to the original version. In fact, the equations involving y could equally well be taken as defining the model.

III. DENSITY-FUNCTION DESCRIPTION

We will begin our analysis by considering the behavior of a system of all-to-all coupled oscillators in the absence of noise. Later, in Sec. IX, we will include the effects of noise. To describe the state of the full population, we use a density function and flux defined by

$$\rho(y, t) = \frac{1}{N} \sum_{i=1}^N \delta(y - y_i(t)) \quad (3.1)$$

and

$$J(y, t) = [E_0 + \Gamma(y)\epsilon(t)]\rho(y, t). \quad (3.2)$$

In the range $0 < y < 1$, these satisfy the continuity equation

$$\frac{\partial \rho}{\partial t} = - \frac{\partial J}{\partial y} \quad (3.3)$$

and, at the end points, the boundary condition

$$J(0, t) = J(1, t), \quad (3.4)$$

expressing the fact that once an oscillator pulses or fires it is reset instantaneously to zero. The quantity $J(1, t)$ is just the average single oscillator firing rate and $\rho(y, t)\Delta y$ is the fraction of neurons with y_i lying between y and $y + \Delta y$ at time t .

The asynchronous solution described in terms of the variable y has $\rho(y)=1$ and $J(y)=E_0$. To investigate whether the asynchronous state is stable we expand around this solution, writing

$$J(y, t) = E_0 + j(y, t). \quad (3.5)$$

We will use the flux J in our computations (in the absence of noise) since the density ρ can be obtained from Eq. (3.2) once J is known. To examine the stability of small fluctuations about the asynchronous firing state we will expand to first order in the quantities $j(y, t)$ and $\epsilon(t)$. In this limit, the continuity Eq. (3.3) becomes

$$\frac{\partial j}{\partial t} = \Gamma(y) \frac{d\epsilon}{dt} - E_0 \frac{\partial j}{\partial y} \quad (3.6)$$

and the coupling variable $\epsilon(t)$ is determined by the equations

$$\frac{d\epsilon}{dt} = -\alpha_1 \epsilon + h \quad (3.7)$$

and

$$\frac{dh}{dt} = -\alpha_2 h + \alpha_1 \alpha_2 j(1, t). \quad (3.8)$$

It is straightforward to verify that Eqs. (3.7) and (3.8) reproduce the coupling response of Eq. (2.2).

IV. STABILITY OF THE ASYNCHRONOUS STATE

To study the stability of the asynchronous state, we look for solutions of the linearized equations with the time dependence of j , ϵ , and h given by $\exp(\lambda t)$. This will allow us to compute the spectrum of eigenvalues λ of the stability matrix [18] (similar methods are used in Refs. [12], [24], and [25]). Solving the first-order continuity Eq. (3.6) with the boundary condition (3.4) gives

$$j(y, t) = \frac{\epsilon(t)\lambda}{E_0} \left[\int_0^y dy' \Gamma(y') e^{\lambda y'/E_0} + C_\lambda \right] e^{-\lambda y/E_0} \quad (4.1)$$

where

$$C_\lambda = (e^{\lambda/E_0} - 1)^{-1} \int_0^1 dy \Gamma(y) e^{\lambda y/E_0}. \quad (4.2)$$

The eigenvalues are determined by substituting this solution into Eqs. (3.7) and (3.8) giving

$$E_0 (e^{\lambda/E_0} - 1) (\lambda + \alpha_1) (\lambda + \alpha_2) = \alpha_1 \alpha_2 \lambda \int_0^1 dy \Gamma(y) e^{\lambda y/E_0}. \quad (4.3)$$

This result allows us to determine the stability properties

and relaxation time constants of the asynchronous state.

Equation (4.3) has an infinite number of solutions giving the full spectrum of eigenvalues of the infinite-dimensional stability matrix. Finding the eigenvalues is, in general, a difficult problem, but if the coupling function Γ is independent of y they can be found easily. We will use this as the basis for various perturbation expansions. If $\Gamma(y)$ is a constant, there is a set of imaginary eigenvalues given (for integer n) by

$$\lambda = 2\pi i n E_0, \quad n \neq 0. \quad (4.4)$$

[Note that for these eigenvalues C_λ is not given by Eq. (4.2), but is determined instead by Eqs. (3.7) and (3.8).] Since these are pure imaginary, the asynchronous state with y -independent coupling is at best marginally stable. In addition to these imaginary eigenvalues, there are eigenvalues

$$\lambda = -\frac{1}{2}(\alpha_1 + \alpha_2) \pm \frac{1}{2}[(\alpha_1 - \alpha_2)^2 + 4\alpha_1\alpha_2\Gamma]^{1/2}. \quad (4.5)$$

In order for the y -independent case to be marginally stable, we must have $\Gamma < 1$. A special case of y -independent coupling is no coupling at all, $\Gamma = 0$, in which case these eigenvalues become simply $\lambda = -\alpha_1$ and $-\alpha_2$.

V. WEAK-COUPLING EXPANSION

We can use the eigenvalues obtained for zero coupling to construct a weak-coupling perturbation expansion for the case of small $\Gamma(y)$. As we have seen, the zero coupling case is marginally stable with the imaginary eigenvalues $\lambda = 2\pi i n E_0$. Small coupling adds a real part to these eigenvalues determining the stability or instability of the asynchronous state. Therefore, we will focus our attention on these imaginary eigenvalues. Since these always come in complex conjugate pairs, we will consider only the eigenvalues with $n > 0$. To first order in Γ , we find that the eigenvalues that were purely imaginary at lowest order become

$$\lambda = 2\pi i n E_0 \left[1 + \frac{\alpha_1\alpha_2(A_n + iB_n)}{(2\pi i n E_0 + \alpha_1)(2\pi i n E_0 + \alpha_2)} \right] \quad (5.1)$$

where

$$A_n + iB_n = \int_0^1 dy \Gamma(y) e^{2\pi i n y}. \quad (5.2)$$

Stability of the asynchronous state requires that the real parts of these eigenvalues be negative or, equivalently (for $n > 0$),

$$B_n(\alpha_1\alpha_2 - 4\pi^2 n^2 E_0^2) > 2\pi n E_0 A_n(\alpha_1 + \alpha_2). \quad (5.3)$$

For large n we find that $B_n \propto 1/n$ and $A_n \propto 1/n^2$ for non-pathological functions $\Gamma(y)$. From this we see that for large n we must have $B_n < 0$, which, from standard theorems on Fourier transforms [26], implies under quite general conditions that

$$\Gamma(1) > \Gamma(0). \quad (5.4)$$

This is algebraically equivalent to the condition

$$\frac{G(0)}{G(1)} < \frac{F(0)}{F(1)}. \quad (5.5)$$

In the limit $\alpha_2 \rightarrow \alpha_1 = \alpha$, if we assume that $B_n < 0$ for all n , we obtain the stability conditions

$$\alpha < 2\pi n E_0 \{ (A_n/B_n) + [1 + (A_n/B_n)^2]^{1/2} \}. \quad (5.6)$$

In many situations, the bound with $n=1$ will be the most restrictive.

As a specific example, we consider a case that is widely used as a simple model neuron,

$$F(x) = k(x_0 - x) \quad (5.7)$$

and

$$G(x) = g(x_E - x) \quad (5.8)$$

where k, g, x_0 , and x_E are constants with x_0 greater than one. A large population of such oscillators has an asynchronous state firing at a rate given in the weak-coupling limit by

$$E_0 \approx k \left[\ln \left[\frac{x_0}{x_0 - 1} \right] \right]^{-1}, \quad (5.9)$$

which can be obtained from Eq. (2.5). For this case, $A_n/B_n = -k/2\pi n E_0$ and in the weak-coupling limit the asynchronous state is stable if

$$x_E > x_0, \quad (5.10)$$

which ensures that $B_n < 0$ and

$$\alpha_1\alpha_2 < 4\pi^2 E_0^2 - k(\alpha_1 + \alpha_2). \quad (5.11)$$

In the limit $\alpha_2 \rightarrow \alpha_1 = \alpha$ this gives

$$\alpha < -k + (k^2 + 4\pi^2 E_0^2)^{1/2}. \quad (5.12)$$

We will address the implications of these results in Sec. VIII.

VI. BEYOND WEAK COUPLING

We can determine the stability of the asynchronous state for the model of Eqs. (5.7) and (5.8) when the coupling constant g is not small either by using another approximate calculation or by numerical computation. We begin with the analytical approach by noting that when $x_E = x_0$, Eq. (2.9) gives a y -independent Γ . If x_E is close to x_0 , we can expand in the small quantity $x_E - x_0$ to compute the corrections to the imaginary eigenvalues $\lambda = 2\pi i n E_0$ for the y -independent case and determine the stability properties as in Sec. V.

If $x_E - x_0$ is small we have

$$\Gamma(y) \approx \frac{gE_0}{\kappa} + \frac{gkE_0(x_E - x_0)}{x_0\kappa^2} e^{\kappa y/E_0} \quad (6.1)$$

where $\kappa = k + gE_0$. From this we can compute the relevant eigenvalues to lowest order in $x_E - x_0$ using Eq. (4.3),

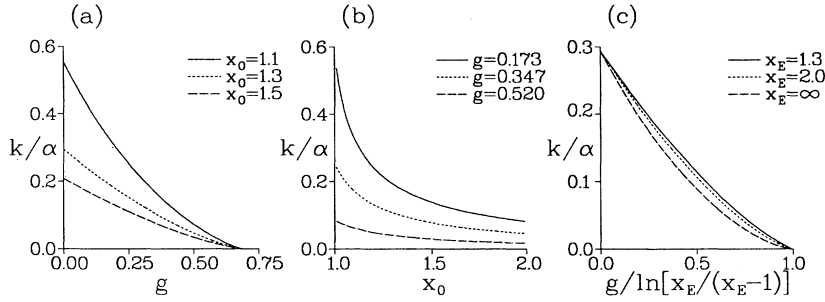


FIG. 1. Boundaries between regions where the asynchronous state is stable and where it is unstable. The stable region is above the lines. (a) The dependence of the coupling time constant $1/\alpha$ (measured in units of k) on g for various values of x_0 with $x_E=2.0$. (b) The dependence on x_0 for various values of g with $x_E=2.0$. (c) The x axis represents a normalized coupling strength chosen to hold the integral of $1/G$ constant. Various values of x_E are shown with $x_0=1.3$.

$$\lambda = 2\pi i n E_0 + \frac{2\pi i n \alpha_1 \alpha_2 g k E_0^3 (x_E - x_0) \kappa^{-2} x_0^{-1} (e^{\kappa/E_0} - 1)}{[\alpha_1 \alpha_2 k / \kappa - 4\pi^2 n^2 E_0^2 + 2\pi i n E_0 (\alpha_1 + \alpha_2)] (\kappa + 2\pi i n E_0)} \quad (6.2)$$

From this result, we find that the asynchronous state will be stable if $x_E > x_0$ as in (5.10) and if

$$\alpha_1 \alpha_2 \left[\frac{k}{k + g E_0} \right] < 4\pi^2 E_0^2 - (k + g E_0) (\alpha_1 + \alpha_2). \quad (6.3)$$

When $\alpha_2 \rightarrow \alpha_1 = \alpha$ we get the stability condition

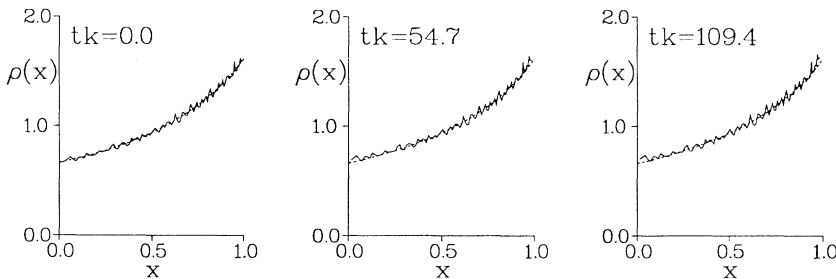
$$\alpha < -\frac{\kappa^2}{k} + \left[\frac{\kappa^4}{k^2} + \frac{4\pi^2 E_0^2 \kappa}{k} \right]^{1/2}. \quad (6.4)$$

In the limit of small g , these results go over to the weak-coupling case considered in Sec. V.

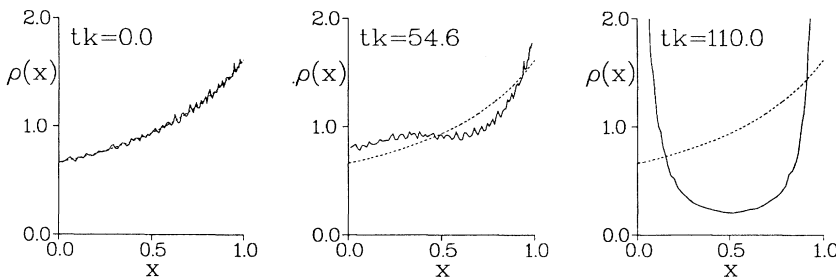
VII. COMPUTER SIMULATIONS AND NUMERICAL SOLUTION

We have also investigated the stability of this model by numerically computing eigenvalues of the stability matrix. The results for the model of Eqs. (5.7) and (5.8) are

(a) $k/\alpha=0.15$



(b) $k/\alpha=0.05$



shown in Fig. 1. For simplicity we plot the case $\alpha_2 \rightarrow \alpha_1 = \alpha$. The vertical axis in Fig. 1 is k/α , which is the coupling time constant measured in units of the oscillator time constant. The lines in the figures indicate the boundary between parameter ranges where the asynchronous state is stable (above the line) and where it is unstable (below the line). Various parameter values and dependences are shown. In the case where we consider different values of x_E we have divided the coupling constant g by $\ln[x_E/(x_E-1)]$ so that the integral of $1/G(x)$ from zero to one is held fixed as x_E is varied for fixed position on the x axis.

In Fig. 2 we compare the mean-field results with a computer simulation of a population of 100 integrate-and-fire oscillators. We estimate the density function from a finite population of N oscillators by using the distribution of x values in the following way. Suppose a given oscillator has the value x_i . From all the oscillators in the population with $x > x_i$, we find the oscillator in the

FIG. 2. Comparison of theoretical prediction with results obtained by simulating 100 integrate-and-fire oscillators. The time of each plot is indicated in units of $1/k$. (a) The value of α was chosen so that the asynchronous state is stable and the simulation results (solid line) match the theoretical prediction (dashed curve). (b) α is larger so that the asynchronous state is unstable. The simulation diverges from the predicted curve for the asynchronous state and the population ultimately goes over to a synchronous firing state. For this figure $x_E=2.0$ and $x_0=1.5$ and $g=0.28$.

population that has its x value nearest to x_i . Similarly we find the oscillator closest to x_i from below. Labeling these two neighboring x values x_{i+1} and x_{i-1} , the amount of x space occupied by the oscillator with $x = x_i$ is $(x_{i+1} - x_{i-1})/2$. We therefore identify the density at the point x_i as

$$\rho(x_i) = \frac{2}{N(x_{i+1} - x_{i-1})}. \quad (7.1)$$

This is compared with the predictions of the mean-field calculation for both a stable and an unstable situation in Fig. 2. In Fig. 2(a) we have used a value of k/α for which the asynchronous state is stable and the density function from the simulations (solid line) accurately matches the predicted function (dashed line). In Fig. 2(b), we chose k/α in the unstable range and as time progresses the observed density function (solid line) diverges from the theoretical curve for the asynchronous solution (dashed line) as the instability grows. From the last panel in Fig. 2(b), it is clear that the system has gone into a synchronous firing state and the system is right in the middle of firing. Further simulations of the type shown in Fig. 2 have convinced us of the validity of our results for the boundary between regions where the asynchronous state is stable and where it is unstable.

VIII. DISCUSSION OF RESULTS

Before considering the effects of noise, we will briefly discuss some of the interesting features of our results to this point. For the model of Eqs. (5.7) and (5.8), we have found that x_E must be greater than x_0 in order for the asynchronous state to be stable. This restricts the types of excitatory coupling that can produce asynchrony and also means that inhibitory interactions (which would typically have $x_E \leq 0$) cannot stabilize the asynchronous state even if they are time delayed, a rather surprising result. Such anti-intuitive effects of inhibitory and excitatory coupling have been noted before. Work on model thalamic networks by Wang and Rinzel [27] has revealed that time-delayed inhibitory interactions can lead to a synchronous state. The reverse effect has also been seen, excitatory, resistive coupling can in some cases produce antiphase synchronization [28]. The other conditions we found for stable asynchronous states such as (5.11) or (6.3) indicate that both a finite rise and fall time are important to stabilize the asynchronous state. In the limit $\alpha_2 \rightarrow \infty$, our interaction function becomes a single exponential with instantaneous rise and exponential fall. Our results indicate that such a model has no stable asynchronous state in the absence of noise.

Note that for large n the real part of the eigenvalues given by Eq. (5.1) or (6.2) is

$$\text{Re}\{\lambda\} \propto -\frac{1}{n^2}. \quad (8.1)$$

The factor of $1/n^2$ implies that the modes with high n will decay very slowly. Thus fluctuations that are of short wavelength in y will be long lived. The ‘‘noise’’ seen in the simulations of Fig. 2 is a result of this

phenomenon. It does not represent noise in the sense of Sec. IX, but rather indicates the presence of modes with high n values that have not yet decayed to zero.

IX. INCLUDING NOISE

We can study the effects of noise on the system of oscillators by including in Eq. (2.7) a randomly fluctuating term $\eta_i(t)$,

$$\frac{dy_i}{dt} = E_0 + \Gamma(y_i)\varepsilon(t) + \eta_i(t) \quad (9.1)$$

satisfying

$$\langle \eta_i(t) \rangle = 0 \quad (9.2)$$

and

$$\langle \eta_i(t)\eta_j(t') \rangle = 2D\delta_{ij}\delta(t-t') \quad (9.3)$$

where $\langle \rangle$ indicates an expectation value. The parameter D determines the magnitude of the noise. In this case, the continuity equation (3.3) becomes the Fokker-Planck equation, which is identical to (3.3) except that J is now given by

$$J(y, t) = \left[E_0 + \Gamma(y)\varepsilon(t) - D \frac{\partial}{\partial y} \right] \rho(y, t) \quad (9.4)$$

rather than by (3.2). Noise can push y_i below zero so the Fokker-Planck equation is now satisfied in the range $y < 0$ and $0 < y < 1$. Boundary conditions are imposed at the excluded points $y=0$ and 1 . The value of y cannot become arbitrarily negative so

$$\rho(-\infty, t) = 0. \quad (9.5)$$

When an oscillator fires after reaching $y_i = 1$ it returns to $y_i = 0$ as before. This means that, although ρ is continuous at the point $y=0$,

$$\rho(0^-, t) = \rho(0^+, t), \quad (9.6)$$

its derivative is discontinuous at this point. The flux through the point $y=0^+$ consists of the flux coming from negative y and that coming from $y=1$ due to resetting. Thus

$$J(0^+, t) = J(0^-, t) + J(1, t). \quad (9.7)$$

An additional boundary condition must be imposed at the point $y=1$. In the presence of noise, all firing is due to noise. In other words, as $y \rightarrow 1$ the probability that the noise term will cause the oscillator to fire approaches one. As a result

$$\rho(1, t) = 0. \quad (9.8)$$

Despite this condition, there is firing at a rate given by

$$J(1, t) = -D \frac{\partial \rho(1, t)}{\partial y}. \quad (9.9)$$

The density function for the asynchronous firing state can be found by solving the time-independent Fokker-Planck equation $dJ/dy=0$ with J given by (9.4) and im-

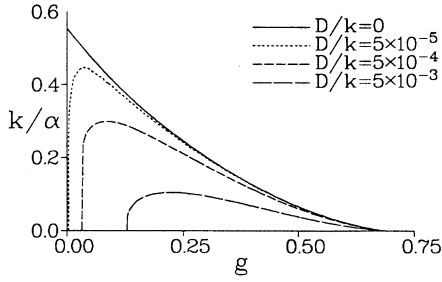


FIG. 3. The effect of noise on the boundary between stable and unstable asynchronous states. The plot is similar to Fig. 1(a). As the noise level increases the boundary gets lower and shifts to the right. $x_E = 2.0$ and $x_0 = 1.1$.

posing the boundary conditions listed above. We find that the flux is equal to the firing rate as before, $J(y, t) = E_0$, and that

$$\rho(y, t) = \rho_0(y) = \begin{cases} e^{E_0 y/D} - e^{E_0(y-1)/D}, & y < 0 \\ 1 - e^{E_0(y-1)/D}, & 0 < y < 1. \end{cases} \quad (9.10)$$

The stability of this state can be determined, as before, by expanding around this solution, considering fluctuations with exponential time dependence, and computing the eigenvalues. If we let $\delta\rho(y, t)$ represent a small fluctuation in $\rho(y, t)$ about the static solution $\rho_0(y)$, then $\delta\rho$ must satisfy the linearized Fokker-Planck equation

$$\frac{\partial \delta\rho}{\partial t} = D \frac{\partial^2 \delta\rho}{\partial y^2} - E_0 \frac{\partial \delta\rho}{\partial y} - \varepsilon \frac{\partial(\Gamma\rho_0)}{\partial y} \quad (9.11)$$

and the eigenvalues are determined by

$$(\lambda + \alpha_1)(\lambda + \alpha_2)\varepsilon = -\alpha_1\alpha_2 D \frac{\partial \delta\rho(1, t)}{\partial y}, \quad (9.12)$$

which arises from Eqs. (3.7) and (3.8).

The computation of the eigenvalues of the stability matrix with noise is similar to the calculation presented in

Sec. IV. Equation (9.11) is solved subject to the boundary conditions listed above and this result is substituted into (9.12) giving

$$E_0(e^{\Lambda/E_0} - 1)(\lambda + \alpha_1)(\lambda + \alpha_2) = \alpha_1\alpha_2\Lambda \int_{-\infty}^1 dy \rho_0(y)\Gamma(y)e^{\Lambda y/E_0} \quad (9.13)$$

with

$$\Lambda = \frac{E_0^2}{2D} [(1 + 4D\lambda/E_0^2)^{1/2} - 1]. \quad (9.14)$$

This equation replaces (4.3) when noise is included. Note that when $D \rightarrow 0$, we recover (4.3) from (9.13) since $\Lambda \rightarrow \lambda$ and $\rho_0 = 1$ for $0 < y < 1$ while $\rho_0 = 0$ for $y < 0$ in this limit.

It is interesting to examine the effect that noise has on the marginally stable asynchronous state that we found for zero coupling. From (9.13) we find that in this case the eigenvalues are given by $\lambda = -\alpha_1$, $\lambda = -\alpha_2$, and $\Lambda = 2\pi i n E_0$, which gives

$$\lambda = 2\pi i n E_0 - 4\pi^2 n^2 D. \quad (9.15)$$

Thus noise stabilizes the asynchronous state as we would expect. Note that modes with large n are more strongly stabilized by noise than those with small n .

Figure 3 shows the effect of various levels of noise on the boundary between the stable and unstable regions for asynchronous firing. As in the preceding figures the model of Eqs. (5.7) and (5.8) is used in the limit $\alpha_{2j} \rightarrow \alpha_1 = \alpha$ and the region above the line is stable and below the line unstable. Noise lowers the boundary line and creates a region at small coupling where even instantaneous coupling allows stable asynchronous firing.

We have seen that in the absence of noise there is no stable asynchronous state with inhibitory coupling or indeed whenever $x_E < x_0$. This is because modes with higher n are increasingly less stable in the inhibitory case, and it is impossible to stabilize all of them. However, the situation is different when noise is present. We see from

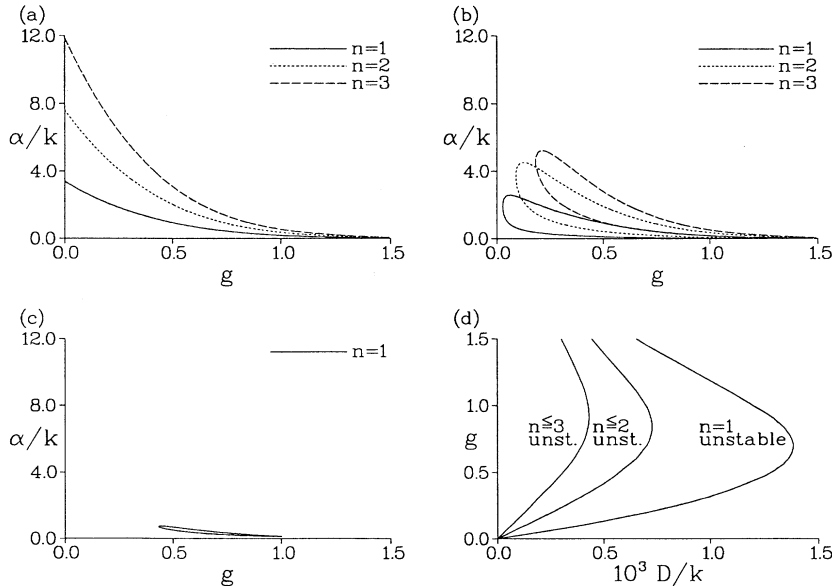


FIG. 4. Stability of the asynchronous state with inhibitory coupling and noise. In (a)–(c) the vertical axis is α/k , which is proportional to the inverse of the coupling time constant. (a) Stability boundaries for the first three modes with inhibitory coupling and no noise. (b) The regions inside the three curves indicate parameter values for which the $n = 1$ –3 modes are unstable in a model with inhibitory coupling and noise. (c) The region inside the boundary show where the $n = 1$ mode is unstable when more noise is added stabilizing the second and third modes. (d) Upper and lower critical values of the coupling strength g as a function of the noise level (in units of $1/k$). To the left of the solid line, the modes indicated are unstable. To the right of all lines the asynchronous state is stable for all values of α/k . For these figures $x_0 = 2.0$, and $x_E = -0.5$ so the coupling is inhibitory.

Eq. (9.15) that noise has a more stabilizing effect when n is larger. Figure 4(a) shows the boundary lines between stable and unstable regions for the first three modes. In this case the vertical axis is α/k , but the stable region is once again above the lines. Note that as n increases the lines of stability get higher and higher. However, in the presence of noise it is possible to stabilize the high n modes. Figure 4(b) shows such a situation. The $n=1-3$ modes are only unstable inside the three regions shown. Outside the regions where the low n modes are unstable, the asynchronous state is completely stable. Figure 4(c) shows that at even higher noise levels the regions where the $n=2$ and 3 modes are unstable have vanished and the $n=1$ mode is only unstable in a small region. Equation (9.15) shows that noise will always stabilize the asynchronous state if the coupling is weak enough. In addition, the unstable regions in Figs. 4(b) and 4(c) do not extend beyond a certain critical value of the coupling strength g . Therefore, for g greater than one critical value or less than another critical value, the asynchronous state will be stable for all values of α/k when we have inhibitory coupling and noise. The upper and lower critical values are plotted for the first three modes in the right panel of Fig. 4(d). To the right of all three lines in Fig. 4(d) the asynchronous state is stable for all values of α/k .

X. IMPLICATIONS FOR FIRING-RATE MODELS

It is interesting to see whether the asynchronous state we have been analyzing can be described by a firing-rate model. We can use our results to compare the behavior of transients about the asynchronous state in the full model using the density $\rho(y,t)$ to describe the population and in a simpler model where the population is described solely by the average firing rate $R(t)=J(1,t)$ and the detailed distribution over y is ignored. Under what conditions is this valid? Our results indicate that for the particular asynchronous state we have studied this is a fairly subtle question.

To construct a firing-rate model [22], we first determine the single oscillator firing rate as a function of the coupling variable $E(t)$ in the static case when $E(t)$ is a constant. We will call this static firing-rate function $R_0(E)$. In the simplest models, the dynamic firing rate $R(t)$ is determined by the equation

$$\frac{dR}{dt} = \alpha_0 [R_0(E) - R] \quad (10.1)$$

where α_0 is a constant. E is given by equations similar to those of the spiking model except that $R(t)$ replaces $J(1,t)$,

$$\frac{dE}{dt} = -\alpha_1 E + H \quad (10.2)$$

with

$$\frac{dH}{dt} = -\alpha_2 H + \alpha_1 \alpha_2 R. \quad (10.3)$$

By construction $R_0(E_0)=E_0$ so the firing-rate model has an asynchronous solution identical to that of the full model. What about the transients about this solution? The full description has an infinite number of transient modes while the firing-rate model has only three with eigenvalues given by

$$(\lambda + \alpha_0)(\lambda + \alpha_1)(\lambda + \alpha_2) = \alpha_0 \alpha_1 \alpha_2 R'_0(E_0) \quad (10.4)$$

where R'_0 is the derivative of R_0 . The best strategy might be to match these eigenvalues to the longest lasting modes of the full model ignoring the more rapidly dying transients. Clearly this will only work for parameter values allowing a stable asynchronous state but even so there is a complication. Figure 5(a) shows the real part of the first four eigenvalues for the full model of Eqs. (5.7) and (5.8). Note that as n increases the real part of the eigenvalue tends to become less negative. Indeed, as we have noted, the real part of the eigenvalues for large n is proportional to $-1/n^2$. Therefore, we cannot simply match the eigenvalues of the firing-rate model to the modes of the full model with the least negative real parts.

We can argue that the firing-rate model provides a coarse-grained description so that transients of $\rho(y,t)$ with rapid variations in y are irrelevant. In this case we would match the eigenvalues of the firing-rate model to the longest wavelength modes of the full model. However, we might still worry about the effect of the higher modes since they are not damped quickly. To apply the firing-rate description we must be assured either that these high n modes will not be excited or that they will have no important effects. The situation is much less murky when noise is present. Noise makes the real parts of the high- n modes more negative. If the noise level is high enough, a situation can arise, as in Fig. 5(b), where the $n=1$ mode is the longest lasting mode. In this case, the justification of a firing-rate description is more straightforward.

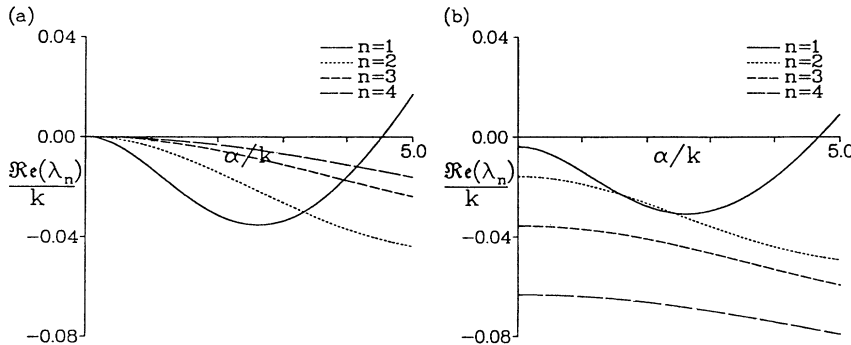


FIG. 5. The real parts of the eigenvalues for the first four modes as a function of α/k . (a) No noise is present and through most of the range the $n=1$ mode has the most negative real part. (b) When noise is added at the level of $D/k = 10^{-4}$, the $n=1$ mode has the least negative real part through most of the range. Here $x_E = 2.0$, $x_0 = 1.1$, and $g = 0.28$.

In summary, the population of oscillators we have studied can be described using a simpler firing-rate model either if (1) sufficient noise is present to rapidly remove the higher modes that are ignored in the firing-rate description or (2) the initial conditions are restricted so that the higher modes with long lifetimes are not excited. Otherwise, the higher n modes, not described by the firing-rate model, will be present and they will not quickly be damped away.

ACKNOWLEDGMENTS

We wish to thank A. Treves for extensive discussions of his work and for helpful comments. In addition, we thank M. Tsodyks, H. Sompolinsky, M. Usher, and S. Strogatz for useful discussions of their related work. This research was supported by the National Institute of Mental Health Grant No. MH46742 and the National Science Foundation Grant No. DMS-9208206.

-
- [1] A. T. Winfree, *J. Theor. Biol.* **16**, 15 (1967).
 - [2] Y. Kuramoto, in *International Symposium on Mathematical Problems in Theoretical Physics*, edited by H. Araki, Lecture Notes in Physics Vol. 39 (Springer, Berlin, 1975); *Chemical Oscillations, Waves and Turbulence* (Springer, New York, 1984).
 - [3] G. B. Ermentrout and N. Kopell, *SIAM J. Math. Anal.* **15**, 215 (1984).
 - [4] G. B. Ermentrout, *J. Math. Biol.* **22**, 1 (1985).
 - [5] S. H. Strogatz and R. E. Mirollo, *J. Phys. A* **21**, L699 (1988); *Physica D* **31**, 143 (1988).
 - [6] H. Daido, *Prog. Theor. Phys.* **81**, 727 (1989); *J. Stat. Phys.* **60**, 753 (1990).
 - [7] P. C. Matthews and S. H. Strogatz, *Phys. Rev. Lett.* **65**, 1701 (1990).
 - [8] L. F. Abbott, *J. Phys. A* **23**, 3835 (1990).
 - [9] R. E. Mirollo and S. H. Strogatz, *SIAM J. Appl. Math.* **50**, 1645 (1990).
 - [10] Y. Kuramoto, *Physica D* **50**, 15 (1991).
 - [11] Y. Kuramoto and I. Nishikawa, *J. Stat. Phys.* **49**, 569 (1987).
 - [12] S. H. Strogatz and R. E. Mirollo, *J. Stat. Phys.* **63**, 613 (1991).
 - [13] R. D. Traub and R. S. W. Wong, *Sci.* **216**, 745 (1983).
 - [14] R. Miles and R. K. S. Wong, *J. Physiol.* **388**, 611 (1987).
 - [15] M. V. Tsodyks, I. Mit'kov, H. Sompolinsky, *Phys. Rev. Lett.* (to be published).
 - [16] C. van Vreeswijk and L. F. Abbott, *SIAM J. Appl. Math.* **53**, 253 (1993).
 - [17] M. Usher, H. Schuster, and E. Niebur, *Neural Comput.* (to be published).
 - [18] A. Treves (unpublished).
 - [19] H. R. Wilson and J. D. Cowan, *Biophys. J.* **12**, 1 (1972).
 - [20] J. J. Hopfield, *Proc. Natl. Acad. Sci. U.S.A.* **79**, 2554 (1982); **81**, 3088 (1984).
 - [21] A. A. Frolov and A. V. Medvedev, *Biophysics* **31**, 332 (1986).
 - [22] L. F. Abbott, in *From Biology to High Energy Physics*, edited by O. Benhar, C. Bosio, P. Del Giudice, and E. Tabet (ETS Editrice, Pisa, 1991).
 - [23] D. J. Amit and M. V. Tsodyks, *Network* **3**, 121 (1991).
 - [24] D. Golomb, D. Hansel, B. Shraim, and H. Sompolinsky, *Phys. Rev. A* **45**, 3516 (1992).
 - [25] S. H. Strogatz and R. E. Mirollo (unpublished).
 - [26] H. S. Carslaw, *Introduction to the Theory of Fourier's Series and Integrals* (Dover, New York, 1983), p. 270.
 - [27] X.-J. Wang and J. Rinzel, *Neuroscience* (to be published).
 - [28] A. Sherman and J. Rinzel, *Proc. Natl. Acad. Sci. U.S.A.* **89**, 2471 (1992).